

Space charge resonances and instabilities in rings.

I. Hofmann, G. Franchetti and A. Fedotov[†]

GSI, 64291 Darmstadt, Germany

[†]BNL, Upton NY 11973, USA

Abstract. We show that the influence of space charge on resonances of coasting beams in circular machines can be discussed in terms of a coherent frequency shift leading to a “coherent advantage”, and of space charge induced resonant instabilities absent in the zero space charge limit. These mechanisms are exemplified for the SNS ring as well as the SIS18 of GSI.

INTRODUCTION

While resonances in circular machines driven by systematic or imperfection lattice terms have been widely explored since the early times of accelerators, the role of space charge has found comparable attention only in recent years [1, 2, 3, 4, 5, 6, 7]. The most obvious effect of space charge is the incoherent tune shift and spread, which leads to an extended foot print of single particle tunes in the tune diagram. Less obvious is the observation that the response on a resonance may be modified by the coherent motion of all or a large fraction of particles. This leads to an additional oscillating force, which must be added to the external forces and may cause a coherent shift of the resonance condition; furthermore a different response is obtained, depending on whether the resonance is crossed from above or below, which was first studied in Ref. [1]. The main point of this paper is to show that a systematic study of space charge effects needs to consider the existence of both, resonances *and* instabilities. Such structure instabilities have been studied earlier in the context of linear transport systems [8], but these findings can be applied also to circular accelerators. Our model is that of a coasting beam or, equivalently, a constant line current beam in an ideal barrier bucket. In usual bunched beams in an rf bucket the combined effect of synchrotron motion and line current variation leads to additional effects due to resonance crossing discussed elsewhere in this conference [9].

COHERENT SHIFT OF RESONANCE

The analytical basis for calculating coherent frequency shifts is the calculation of eigenfrequencies for charge density oscillations with arbitrary tune and emittance ratios, hence fully anisotropic beams, by using the dispersion relations derived in Ref. [3] for KV beams and in smooth approximation. These eigenmodes can be excited resonantly in a circular accelerator by appropriate external field perturbations (for round isotropic beams see also Ref. [5]); furthermore, they can be excited by space

charge itself, or a combination of both. Hence, the coherent space charge contribution leads to a shifted condition of resonance of the *coherent* frequency ω with a field perturbation at harmonic n according to

$$\omega = m v_x + l v_y + \Delta\omega = n. \quad (1)$$

Here we express the “mode tune” ω in units of the revolution frequency similar to single particle tunes, and introduce $\Delta\omega$ as coherent shift due to the resonant density oscillations. The importance of such a shift was first pointed out by Smith [10] for second order, and extended to any order by Sacherer [11]. Numerically, it was demonstrated in Ref. [1] – using particle-in-cell simulation – for an example of fourth order resonance crossing.

In order to more easily quantify the effect of the coherent shift, a coherent mode coefficient C_{mk} defined by the equation $n = m(v_0 - C_{mk}\Delta v)$, thus including the incoherent *and* coherent space charge effect, was proposed in Ref. [4] for isotropic beams and uncoupled modes, based on the dispersion equations of Ref. [3]. Here m is denoting an azimuthal, and k a radial mode number, while $\Delta v = v_0 - v$. The radial mode number reflects the order of the perturbed space charge potential; the azimuthal one gives the multiple of v_0 for vanishing space charge. Note that for non-KV beams v and Δv must be understood as rms values. C_{mk} can thus be interpreted as coefficient of attenuation of the single particle space charge shift Δv by the coherent motion, provided that $C < 1$. The intensity can thus be increased by the factor $1/C$ compared with the single particle based resonance condition, which expresses the “coherent advantage”. For the symmetric breathing mode the result is $C = 1/2$, which reflects the strong density perturbation by the cross sectional breathing. This allows increasing Δv by a factor 2 compared with the corresponding single particle resonance condition $n = 2v$; for the quadrupolar mode the coefficient is only $3/4$, hence an allowed intensity increase by the factor $4/3$. The general case for split horizontal and vertical tunes (also unequal emittances) leads to a coefficient C close to the arithmetic mean, e.g. $5/8$, for both modes, hence a “coherent advantage” by the fac-

tor 1.6. In fourth order we find that $C \approx 0.87$ is a good approximation for a broad variation of tune splitting and emittance ratios. This implies a weakening of the “coherent advantage” if fourth order resonances are expected to play a role. We note here that modes with $C > 1$ may appear, in principle, as solutions of the analytical KV-based dispersion relations. Following the discussion in Ref. [12] they should, however, be discarded as artifact of KV-distributions associated with “negative energy”.

SECOND ORDER RESONANCES APPLIED TO SNS

We first discuss the appearance of an imperfection driven second order resonance for the fictitious un-split working point $(v_{0x}, v_{0y}) = (4.6, 4.6)$ driven by a harmonic $n = 9$ gradient error. The effect of the error resonance depends primarily on the tune and not the details of the focusing lattice, hence we can assume a constant focusing for simplicity. The expected resonance condition is

$$2v_x + \Delta\omega = 9. \quad (2)$$

An anti-symmetric error in x and y (as would be produced by a single quadrupole) then drives a quadrupolar mode resonance, whereas a symmetric error is needed to drive the breathing mode resonance. Note that for sufficiently split tunes a single quadrupole error will drive both modes. We assume equal emittances in x and y , and solve the envelope equations with a symmetric relative gradient error Fourier harmonic of 0.001 at $n = 9$ as well as a small initial envelope mismatch of 2%. If the single particle tune is exactly on resonance there is only a small beating of the envelope due to proximity of the coherent resonance (Fig. 1 top). The resonance of the in-phase mode should be expected at $v_{x,y} = 4.4$ based on the calculated value for C . At this value, in fact, the envelope response is significant though not yet maximum (Fig. 1 bottom). The complete picture is shown in Fig. 2 for both, symmetric and anti-symmetric gradient errors. Due to the nonlinear nature of the envelope response the maximum is reached for even slightly stronger tune depression, with a sharply dropping response beyond. As expected, the zero-current case has infinite response at $v_{x,y} = 4.5$. For the actual simulation the particle-in-cell ORBIT code was applied to the SNS lattice with a working point $(v_{0x}, v_{0y}) = (6.45, 4.6)$. The response to an error in a single quadrupole leads to a similar behavior of a shifted curve and steeply dropping maximum envelope slightly beyond the envelope resonance condition. Results for the out-of-phase mode excited by crossing the resonance condition in the y -plane are shown in Fig. 3, where intensity is plotted in terms of a normalized tune shift defined as actual space charge tune shift relative to the distance of the bare tune from the half-integer, i.e.

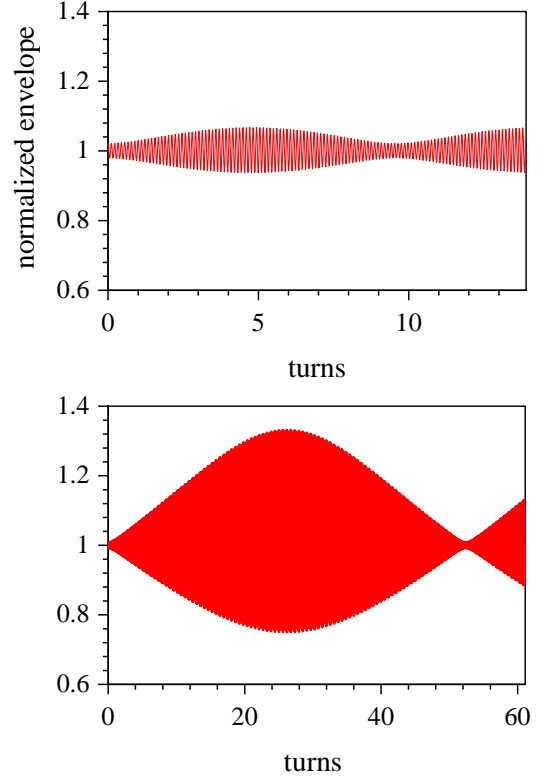


FIGURE 1. In-phase mode envelope evolution at the single particle resonance condition $v_{x,y}=4.5$ (top), and at the point of coherent resonance, $v_{x,y}=4.4$ (bottom) for $v_{0,x,y}=4.6$.

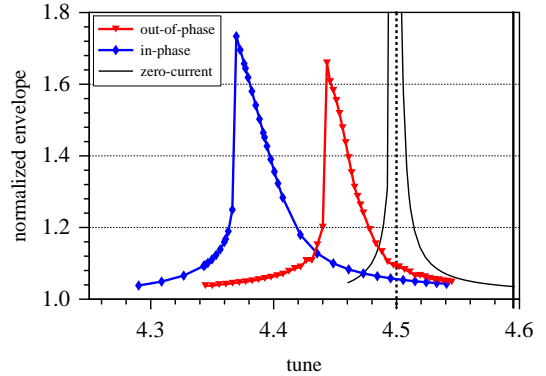


FIGURE 2. Maximum envelope response (normalized to initial envelopes) for both eigenmodes and bare tune $v_{0,x,y}=4.6$ as function of depressed incoherent tune.

$\Delta v_{sc}/\Delta v_{inc}$. The solid vertical line indicates the coherent resonance condition, where the normalized tune shift equals $1/C$, the long-dashed the r.m.s. incoherent resonance condition, and the short-dashed line the incoherent limit due to the small-amplitude particles in a waterbag distribution. As with the simple envelope model above, we find again that the resonance happens at significantly

higher intensity than for single particles in good agreement with the theoretical expectations. In this context the

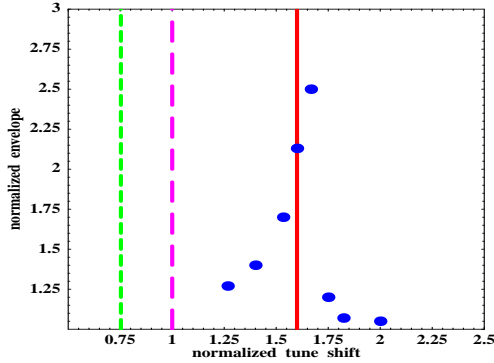


FIGURE 3. Maximum envelope response for SNS lattice as function of normalized tune shift and for $v_{0x}, v_{0y} = (6.45, 4.6)$.

question arises, if fourth order resonances might play a role over the 10^3 turns required for filling the ring. For the typical value of $C = 0.87$ the corresponding normalized tune shift would only be 1.15, hence nearly canceling the second order “coherent advantage”.

RESONANCE AND INSTABILITY FOR THE SIS18

We next consider the working diagram of the SIS18 lattice with 12 super periods and triplet focusing. In Fig. 4 we indicate the usual fourth order systematic single-particle resonance line $4v_y = 12$, its coherent counterpart given by $4v_y + \Delta\omega = 12$ (dotted), which nearly coincides with the lower harmonic of the fourth order coherent resonance $2v_y + \Delta\omega = 12/2$; furthermore the coherent second order resonance condition $2v_y + \Delta\omega = 6$, which could be excited by a 6-th harmonic imperfection gradient error (not studied here). The coherent shifts are calculated for an incoherent space charge tune shift $\Delta v_y = 0.4$ and found practically independent of v_{0x} .

In Table 1 we summarize analytically calculated coherent mode coefficients relevant for the resonances in Fig. 4. They are practically independent of both tunes provided that the incoherent shift is not comparable with or larger than the tune splitting between x and y , in which case corrections are needed.

TABLE 1. Some coherent mode coefficients C for different emittance ratios.

$\varepsilon_x/\varepsilon_y$	2^{nd}	4^{th} / resonance	4^{th} / instability
4	0.66	0.88	0.87
1	0.61	0.85	0.89

For the simulation study we have employed the MICROMAP 2D particle-in-cell code employing 5×10^4 simulation particles on a 128×128 rectangular grid with

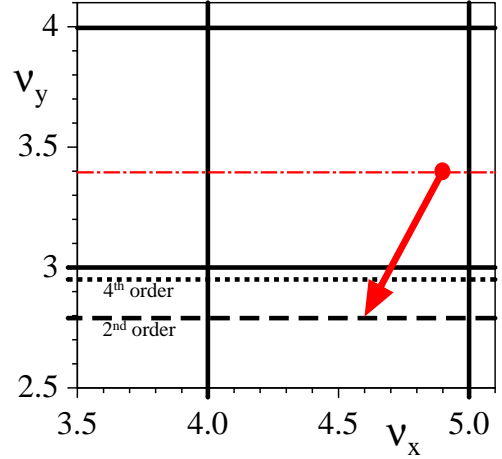


FIGURE 4. Incoherent and coherent shifted resonance lines of SIS18 for fixed $v_{0y}=3.4$ and variable v_{0x} .

conducting boundary conditions [13]. We have used rms matched waterbag distributions generated by filling a 4D hyper-ellipsoid uniformly and deforming it according to the rms matching. Carrying out the self-consistent simulation with $v_{0x} = 4.9$ (which is relatively arbitrary in this context) and $v_{0y} = 3.4$ we find in Fig. 5 that there is a significant emittance growth in y in the region $2.7 < v_y < 2.95$. In fact, we expect two distinct mechanisms to play a role and cause this broad a stop-band. Firstly, the structure envelope instability described by the equation $2v_y + \Delta\omega = 12/2$ is expected. It is characterized by a phase advance of 180° of the underlying envelope mode per focusing period, hence a 1:2 (half-integer) relationship between mode and lattice periodicity; secondly we expect a structural fourth order resonance or instability. Such structure instabilities for sec-

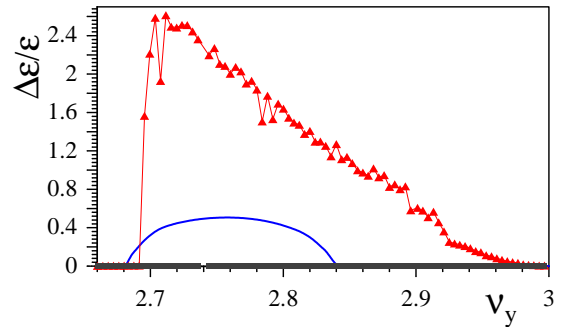


FIGURE 5. Saturated r.m.s. emittance effect after 200 turns in an ideal linear lattice with $v_{0x}, v_{0y} = (4.9, 3.4)$ as function of v_y ($\varepsilon_x/\varepsilon_y=4$). Also shown is $10x(\lambda-1)$ of the theoretical envelope instability growth factor λ .

ond and higher order have been systematically explored for periodic axi-symmetric transport systems in Ref. [8]. These findings apply equally to rings with different focusing in x and y with appropriately modified resonance

conditions. Thus, it is sufficient for an instability of the envelopes to have the zero current phase advance per period sufficiently close to, but above 90° in at least one of the directions. In order to confirm the appearance of an envelope instability we have used the envelope eigenvalue solver KVXYG [14] and found that the present linear lattice with a zero-current phase advance per cell $\sigma_{0y} = 110^\circ$ is subject to envelope instability in the region $2.68 < \nu_y < 2.84$, with an associated envelope growth per cell by a factor λ . This permits us to associate the first part of the simulation stop-band with this mode, while the rest of the simulation stop-band can be only due to the structural fourth order resonance or instability as predicted analytically in Fig. 4 and Table 1. To verify the fourth order nature in this part of the stop-band we show in Fig. 6 the associated structure in phase space for $\nu_y = 2.86$ at an early and a more advanced stage. Note

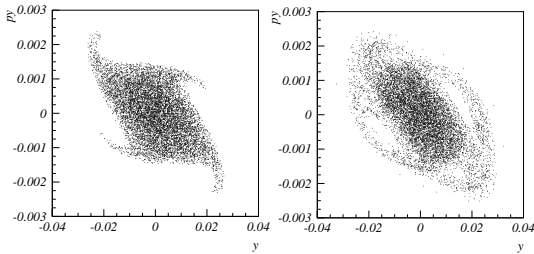


FIGURE 6. Phase space projections in y for fourth order structural response and $\nu_y=2.86$ after turn 2 and 30.

that the location of the coherent fourth order resonance was calculated as $\nu_y \approx 2.95$ in Fig. 4, hence close to the right edge of the simulation stop-band. The asymmetry of the latter is a general nonlinear feature of resonances with significant space charge already identified in the nonlinear envelope simulation of Fig. 1. It is a combined effect of the tune spread existent in a waterbag simulation as well as the space charge detuning effect associated with emittance growth of the fraction of particles on resonance. There is still an effective “coherent advantage” of about 50% compared with the single-particle resonance picture, where one expects the small amplitude particles of a waterbag to be on resonance for $\nu_y < 3.1$.

In our case of strongly split tunes we find that the instability has almost no effect in the x -direction. In order to distinguish between resonances and instabilities we point out that in case of a resonance the driving term is assumed to be given by the lattice or by the space charge of the matched beam; for instabilities the driving term initially exists only on the noise level, but rises – under resonant conditions – exponentially in time. A characteristic feature of such instabilities is their complete absence in the zero-current case. In contrast, the second order resonance $2\nu_y + \Delta\omega = n$, which could be

driven by a $n = 6$ imperfection gradient term would not be distinguishable from the envelope instability in our example, but it would be observable in the zero current limit, where the envelope instability vanishes. A more complete study of second order resonances and the envelope instability in rings (including a weak imperfection driven envelope instability) is found in Ref. [7]. For the fourth order mode above we postulate the simultaneous presence of resonance driven by the structural fourth order term in the waterbag space charge potential, and of structural instability – which may exist near $\sigma_{0y} = 90^\circ$ following Ref. [8] – similar to the self-consistent “Montague resonance” of the next section.

THE “MONTAGUE RESONANT INSTABILITY”

An important case of coupling resonance driven by space charge only is the well-known “Montague resonance”, a fourth order difference resonance first studied in Ref. [15]. It can be seen in a simplified way as a resonance driven by the zero-th harmonic of a quartic term in the space charge potential of a non-uniform beam. In machines with noticeably larger horizontal than vertical emittance it may lead to an exchange of emittances and possibly loss due to vertical acceptance limitation. It has been found in a number of synchrotrons and usually avoided by choosing a large enough tune split. For a recent detailed experimental study see Ref. [16].

The original analysis by Montague was based on a single particle approach using a “frozen-in” space charge potential defined by the initial Gaussian distribution, which neglects the effect of the induced time-varying collective space charge force. It is, however, adequately described only by a coherent resonance condition of the type $2\nu_x - 2\nu_y + \Delta\omega = 0$. The self-consistent simulation explored in detail in Ref. [17] shows, however, that this case is in reality a combination of instability and resonance: it develops as a pure instability for a KV distribution, which has no initial driving nonlinearity as is shown in Fig. 7 (top) for $\nu_y/\nu_{0y} = 0.8$ and $\epsilon_x/\epsilon_y = 2$. In this simulation the focusing ratio was re-defined for each data point such as to obtain a scan over a range of tune ratios. Note that for equal emittances the KV distribution leads to a symmetric loop around $\nu_x/\nu_y = 1$ as was recently shown in a study related to the SNS [18]. The initial growth for the KV-case is found to be exponential, starting from noise level (see Ref. [17]).

An initial waterbag distribution, instead, has all features of a space charge driven resonance due to the presence of a finite nonlinearity from the beginning (bottom of Fig. 7). The instability is, however, still superimposed on the resonance phenomenon. We conclude this by comparing it with a case, where the initial wa-

terbag space charge distribution is “frozen-in”: the maximum emittance exchange reaches only half the amount shown in Fig. 7 due to absence of a coherent response. Effective exchange occurs for specific tune ratios shifted

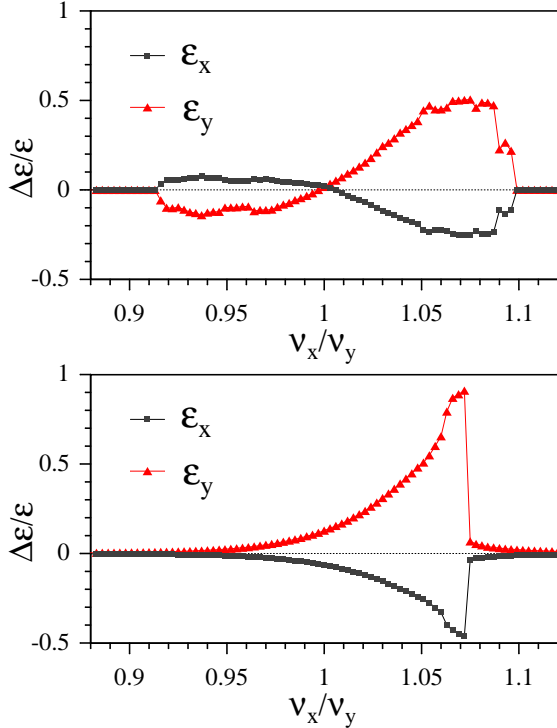


FIGURE 7. Saturated emittance exchange for KV (top) and waterbag (bottom) initial distributions, with $\nu_y/\nu_{0y} = 0.8$, $\epsilon_x/\epsilon_y = 2$, as function of ν_x/ν_y .

from the single particle condition $2\nu_x - 2\nu_y = 0$ due to space charge. It can be shown [17] that maximum growth rates as well as the width of the stop-band are roughly proportional to $\Delta\nu$, while the detailed shape of exchange profiles and maximum emittance exchange are nearly independent of $\Delta\nu$. This enables us to construct a stop-band within the usual tune diagram of a circular machine, which is shown in Fig. 8 for weakly split working points (arbitrary integer parts), using the data of the waterbag simulation in Fig. 7. The asymmetry of the stop-band with respect to the single particle condition $2\nu_x - 2\nu_y = 0$ (dotted line in Fig. 8) is due to the coherent space charge effect and the fact that $\epsilon_x > \epsilon_y$. Note that the width of the stop-band for the waterbag case shrinks to zero for equal emittances; in this limit there is no energy to exchange. The strongest growth of ϵ_y is actually closer to $2\nu_{0x} - 2\nu_{0y} = 0$ than to $2\nu_x - 2\nu_y = 0$.

CONCLUSION

We have found good agreement of space charge induced shifts of resonances between self-consistent simulation

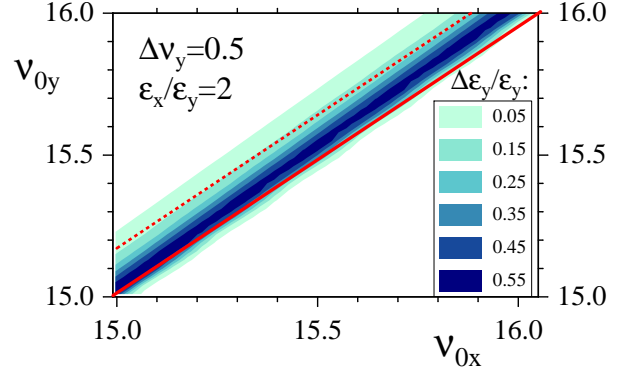


FIGURE 8. Stop-band of self-consistent Montague resonance: color scales indicate saturated growth of the originally smaller emittance in units of $\Delta\epsilon_y/\epsilon_y$.

and analytical theory results and confirmed the existence of resonant instabilities in second and fourth order. Both are shown to give rise to a significant “coherent advantage”, which should be useful for bunch compression in SIS18 near $\nu_y = 3$. These studies also increase our confidence in the simulation codes and should be considered as a basis for further more systematic studies.

REFERENCES

1. I. Hofmann and K. Beckert, *IEEE Trans Nucl. Sci.* **32**, 2264 (1985).
2. S. Machida and M. Ikegami, *AIP Conf. Proc.* 448 (New York, 1998), p. 73
3. I. Hofmann, *Phys. Rev.* **E 57**, 4713 (1998).
4. R. Baartman, *AIP Conf. Proc.* 448 (New York, 1998), p. 56
5. M. Venturini and R.L. Gluckstern, *Phys. Rev. ST Accel. Beams* **3**, 034203 (2000).
6. S. Strasburg and R.C. Davidson, *Phys. Rev.* **E 61**, 5753 (2000).
7. A.V. Fedotov and I. Hofmann, *Phys. Rev. ST Accel. Beams* **5**, 024202-1 (2002).
8. I. Hofmann, L.J. Laslett, L. Smith and I. Haber, *Part. Accel.* **13**, 145 (1983).
9. G. Franchetti and I. Hofmann, these Proceedings
10. L. Smith, Proc. of the Conference of High Energy Accelerators, Dubna, 1963 (AEC, Oak Ridge, TN, 1965), p. 1235.
11. F. Sacherer, Ph.D. thesis, University of California (Lawrence Radiation Laboratory Report UCRL-18454, 1968, unpublished)
12. I. Hofmann, *Part. Acc.* **10**, 253 (1980)
13. G. Franchetti, I. Hofmann, and G. Turchetti *AIP Conf. Proc.* **448**, 233 (1998); ed. A.U. Luccio and W.T. Weng.
14. J. Struckmeier, private communication
15. B.W. Montague, CERN-Report No. 68-38, CERN, 1968.
16. I. Sakai et al., these Proceedings
17. I. Hofmann and O. Boine-Frankenheim, *Phys. Rev. Lett.* **87**, 034802 (2001).
18. A.V. Fedotov, J.A. Holmes and R.L. Gluckstern, *Phys. Rev. ST Accel. Beams* **4**, 084202 (2001)